

# Toxicity evaluation of boron nitride nanospheres and water-soluble boron nitride in *Caenorhabditis elegans*

Ning Wang<sup>1</sup>  
Hui Wang<sup>2</sup>  
Chengchun Tang<sup>3</sup>  
Shijun Lei<sup>1</sup>  
Wanqing Shen<sup>1</sup>  
Cong Wang<sup>1</sup>  
Guobin Wang<sup>4</sup>  
Zheng Wang<sup>1,4</sup>  
Lin Wang<sup>1,5</sup>

<sup>1</sup>Research Center for Tissue Engineering and Regenerative Medicine, Union Hospital,

<sup>2</sup>Department of Medical Genetics, Tongji Medical College, Huazhong University of Science and Technology, Wuhan, <sup>3</sup>Boron Nitride Research Center, School of Materials Science and Engineering, Hebei University of Technology, Tianjin, <sup>4</sup>Department of Gastrointestinal Surgery, <sup>5</sup>Department of Clinical Laboratory, Union Hospital, Tongji Medical College, Huazhong University of Science and Technology, Wuhan, China

Correspondence: Lin Wang;  
Zheng Wang  
Department of Gastrointestinal Surgery;  
Department of Clinical Laboratory,  
Union Hospital, Tongji Medical College,  
Huazhong University of Science and  
Technology, 1277 Jiefang Avenue,  
Wuhan 430022, China  
Email lin\_wang@hust.edu.cn;  
zhengwang@hust.edu.cn

**Abstract:** Boron nitride (BN) nanomaterials have been increasingly explored for potential biological applications. However, their toxicity remains poorly understood. Using *Caenorhabditis elegans* as a whole-animal model for toxicity analysis of two representative types of BN nanomaterials – BN nanospheres (BNNs) and highly water-soluble BN nanomaterial (named BN-800-2) – we found that BNNs overall toxicity was less than soluble BN-800-2 with irregular shapes. The concentration thresholds for BNNs and BN-800-2 were 100 µg·mL<sup>-1</sup> and 10 µg·mL<sup>-1</sup>, respectively. Above this concentration, both delayed growth, decreased life span, reduced progeny, retarded locomotion behavior, and changed the expression of phenotype-related genes to various extents. BNNs and BN-800-2 increased oxidative stress levels in *C. elegans* by promoting reactive oxygen species production. Our results further showed that oxidative stress response and MAPK signaling-related genes, such as *GAS1*, *SOD2*, *SOD3*, *MEK1*, and *PMK1*, might be key factors for reactive oxygen species production and toxic responses to BNNs and BN-800-2 exposure. Together, our results suggest that when concentrations are lower than 10 µg·mL<sup>-1</sup>, BNNs are more biocompatible than BN-800-2 and are potentially biocompatible material.

**Keywords:** boron nitride nanomaterials, *Caenorhabditis elegans*, nanotoxicology, reactive oxygen species, toxicity

## Introduction

An increasing number of engineered nanomaterials (ENMs) have been explored for diverse biomedical applications.<sup>1</sup> Among these ENMs, boron nitride (BN) NMs (also known as “white graphene”)<sup>2</sup> with a structure analogous to carbon NMs have been studied for drug delivery, tissue regeneration, and fluorescent-cell imaging.<sup>3–5</sup> Hydrophobic BN nanospheres (BNNs) and highly water-soluble BN powder (BN-800-2) with irregular shapes are two representative forms of BN NMs. BNNs can be utilized to deliver cytosine–phosphate–guanine oligonucleotides and peptides into lysosomes after cellular uptake;<sup>6–8</sup> similarly, BN-800-2 with high surface area and loading capacity also possesses the potential of being a drug-delivery vehicle.<sup>9</sup> Despite their potential value in biomedicine, BN NMs’ biocompatibility, a key feature fundamentally important for their biomedical application, is poorly understood, with conflicting evidence in the literature.<sup>3,10,11</sup> For instance, some studies claim that BN nanotubes (NTs) and hexagonal BN are more cytocompatible than their carbon counterparts in vitro and in vivo,<sup>3,4,12,13</sup> whereas other studies report otherwise,<sup>10</sup> suggesting that further exploration on BN NM cytotoxicity is needed.

*Caenorhabditis elegans* is a self-reproducing free-living nematode species.<sup>14</sup> As a sensitive and cost-efficient whole-animal model with a short life cycle, *C. elegans* complements mammalian models<sup>15–18</sup> for assessing the toxicity of NMs at the organism or population level.<sup>19–21</sup> These NMs include metal nanoparticles (NPs; TiO<sub>2</sub>, Al<sub>2</sub>O<sub>3</sub>, and ZnO<sub>2</sub>)<sup>22–24</sup> and carbon NPs (carbon NTs [CNTs], graphene oxide [GO], and graphite nanoplatelets).<sup>25–28</sup>

Here, we analyze the two aforementioned representative forms of BN NMs in *C. elegans*: BNNSs and BN-800-2. In this study, we examined the multiple phenotypic toxicities of two types of BN NMs with different morphology, size, and solubility using *C. elegans* in aqueous media. The toxic effects and dosage thresholds were assessed and determined by the exposure of worms to BNNSs or BN-800-2. The life span (lifetime), growth (length of worms), progeny (reproductive number), oxide-stress level, and material distribution were quantitatively analyzed as phenotypic indicators in BNNS- or BN-800-2-exposed worms. The relevant *C. elegans* mutants were employed to investigate the molecular mechanisms underlying the in vivo toxicity of BNNSs and BN-800-2.

## Materials and methods

### Preparation and characterization of BN-based nanomaterials

BNNSs and highly water-soluble BN-800-2 NM were kindly provided by Professor Tang (School of Materials Science and Engineering, Hebei University of Technology, Tianjin, China). In brief, BNNSs were synthesized by chemical deposition to an average diameter of approximately 150 nm per particle, detected by transmission electron microscopy (TEM, H-700FA, 75 kV; Hitachi, Tokyo, Japan) as previously reported.<sup>29</sup> BN-800-2 was synthesized by a thermal substitution reaction of carbon atoms in graphitic carbon nitrides in accordance with a previous method.<sup>9</sup> BNNSs and BN-800-2 at a concentration of 1,000 µg·mL<sup>-1</sup> were stocked stably in K medium (distilled, deionized water with 10 mM NaOAc, 50 mM NaCl, 30 mM KCl, pH 5.5), a liquid medium for maintaining *C. elegans*, at 4°C. The working solution (1–500 µg·mL<sup>-1</sup>) was prepared by diluting the stock solution with K medium at room temperature. The pH value was then readjusted to 5.5. Dynamic light scattering and ζ-potential of BN materials at a concentration of 10 µg·mL<sup>-1</sup> in water or K medium were measured with a Nano Zetasizer system (ZEN 3600; Malvern Instruments, Malvern, UK) at room temperature (Table 1). The stock solution of 1,000 µg·mL<sup>-1</sup> was dispersed in Milli-Q water after sonication for 30 minutes and stored at 4°C. All chemicals were purchased from Sigma-Aldrich (St Louis, MO, US).

**Table 1** Characterizations of BN nanomaterials (mean ± SD)

Characterization	BNNS	BN-800-2
Particle size (nm) <sup>a</sup>	150	~700
Hydrodynamic size in water (nm) <sup>b</sup>	476.5±81.32	238.9±48.74
Hydrodynamic size in K medium (nm) <sup>b</sup>	504.7±57.56	233.5±94.14
Surface charge in water (mV) <sup>b</sup>	-14.9±3.56	-16.6±7.04

**Notes:** <sup>a</sup>Measured by TEM; <sup>b</sup>determined through DLS.

**Abbreviations:** BNNS, boron nitride nanosphere; BN-800-2, highly water-soluble boron nitride; TEM, transmission electron microscopy; DLS, dynamic light scattering.

## Worm culture

*C. elegans* wild-type N2, transgenic strains of *oxIs12* [*UNC47::GFP*; *LIN15(+)*], *jcIs1* [*AJMI::GFP*], and mutant stains of *GAS1* (fc21), *MEK1* (ks54), *PMK1* (km25), *SOD2* (ok1030), and *SOD3* (gk235) were purchased from the Caenorhabditis Genetics Center at the University of Minnesota (Minneapolis, MN, US). They were maintained on nematode growth-medium agar plates and fed with *Escherichia coli* strain OP50 at 20°C as per a standard protocol.<sup>14</sup> For the age-synchronized test, gravid *C. elegans* were eluted and lysed by a standard hypochlorite procedure.<sup>30</sup> L1-stage or L4-stage larvae from an age-synchronized culture were exposed in 24-well sterile tissue plates shaken at 20°C, which were covered with aluminum foil to diminish the potential influence of light. Each well contained 500 µL aliquot of test solution based on K medium (pH 5.5)<sup>31</sup> for all the assays with shaking.

## Larval growth, reproduction, and life-span assays

For the following tests, age-synchronized worms were transferred into 24-well sterile tissue plates with sufficient *E. coli* OP50 in K medium as previously described. BNNSs and BN-800-2 were prepared at final concentrations of 0, 1, 10, 100, and 500 µg·mL<sup>-1</sup>. For larval growth assays, body size at the flat surface area along the anterior–posterior axis of *C. elegans* from L1 larvae was shot every 24 hours for 3 successive days. Then, the *C. elegans* specimens were observed by bright-field microscopy (BX53 equipped with an XM10 digital microscope camera and CellSens Entry imaging software; Olympus, Tokyo, Japan) and measured with ImageJ Express software. At least ten replicates were employed for each assay in three independent tests. For progeny assays, one single synchronized L4-stage larva was placed into an individual well of 24-well sterile tissue plates.<sup>32</sup> The parent *C. elegans* specimens were transferred into a new well every 1.5 days. All embryos and larvae were counted after the transfer under stereo-zoom microscopy (SZX7; Olympus), and ten replicates were employed for each assay.

To determine the lifespan of *C. elegans* exposed to BNNSs or BN-800-2, 30 L4-stage larvae were transferred into a fresh well, with treatments conducted every day during the brood period. The viability of each nematode was verified under stereo-zoom microscopy. Worms without pharyngeal bulb pumping or responding to a gentle blow with a micropipette were scored as dead.

## Locomotion-behavior assays

Locomotion behaviors of worms were appraised by head-thrash and body-bend tests, performed as previously described.<sup>33,34</sup> *C. elegans* exposed to BNNSs or BN-800-2 at different concentrations were drawn out and washed with K medium. Each worm was transferred into 60  $\mu$ L K medium on the surface of agar in a sterile tissue plate and observed under stereo-zoom microscopy. A thrash was defined as a direction change of swing worms at the mid-body. The head thrashes were scored for 1 minute after a recovery period of 1 minute. For body-bend counting, animals were packed onto an empty agar plate and body bends counted for 20 seconds. A body bend was defined as a change in the direction of the posterior bulb of the pharynx along the body axis, assuming that the worm was crawling perpendicularly to the body axis. Fifteen animals were detected per treatment in three independent tests.

## Visualization of $\gamma$ -aminobutyric acid motor neurons

$\gamma$ -Aminobutyric acid (GABA) motor neurons were analyzed using an *oxIs12* transgene strain expressing GFP-fused UNC47 protein. L4-stage larvae were exposed to 500  $\mu$ g·mL<sup>-1</sup> BNNSs or BN-800-2 in K medium on a shaker for 24 hours. Relative green fluorescence was examined with fluorescence microscopy (IX71 equipped with a DP73 digital microscope camera and CellSens Entry imaging software; Olympus) at 488 nm excitation wavelength and 510 nm emission filter. The average integrated optical density of green fluorescence (integrated optical density divided by area) was semiquantified with Image-Pro Plus 6.0 software. Thirty *C. elegans* specimens for each group were counted.

## Reactive oxygen species-production assays

After exposure of BNNSs or BN-800-2 at final concentrations of 0, 1, 10, 100, and 500  $\mu$ g·mL<sup>-1</sup> in K medium on a shaker for 24 hours, the examined L4-stage larvae were washed three times and incubated with 500  $\mu$ L M9 buffer (3 g KH<sub>2</sub>PO<sub>4</sub>, 6 g Na<sub>2</sub>HPO<sub>4</sub>, 5 g NaCl, 1 mL 1 M MgSO<sub>4</sub>, H<sub>2</sub>O to 1 L)

containing 100  $\mu$ g·mL<sup>-1</sup> of 2',7'-dichlorodihydrofluorescein diacetate (Sigma-Aldrich) for 3 hours at 20°C away from light. Tested *C. elegans* specimens were taken out and washed three times with M9 buffer and then examined under fluorescence microscopy at 488 nm excitation wavelength and 510 nm emission filter. The average integrated optical density of green fluorescence (integrated optical density divided by area) was semiquantified with Image-Pro. Fifty *C. elegans* specimens for each group were counted.

## Quantitative real-time polymerase chain reaction

For quantitative real-time polymerase chain reaction (qRT-PCR) analysis, approximately 500 *C. elegans* specimens were exposed to 500  $\mu$ g·mL<sup>-1</sup> of BNNSs or BN-800-2 for 24 hours. Total RNA (~1  $\mu$ g) of worms was extracted using RNAiso Plus (Takara Bio, Kusatsu, Japan) and reverse-transcribed into cDNA using Moloney Murine Leukemia Virus (M-MLV) reverse transcriptase (Vazyme Biotech, Nanjing, China) with oligo-dT primer (Takara Bio). The qRT-PCR was carried out using a StepOnePlus RT-PCR System (Thermo Fisher Scientific, Waltham, MA, US) and operated at optimized annealing temperature of 56°C for 40 cycles. The design of primers was based on the *C. elegans* database ([www.wormbase.org](http://www.wormbase.org)) and blasted in the NCBI database ([www.ncbi.nlm.nih.gov](http://www.ncbi.nlm.nih.gov)). The cycle of threshold (Ct) value of each sample was normalized by subtracting the mean Ct value of actin, as internal reference, and calculated into the relative-quantification fold change compared with the control group by an improved mathematical model.<sup>35</sup> Three independent replicates with three technical replicates were managed for all the tests.

## Biodistribution of BNNSs and BN-800-2 in *C. elegans*

To investigate the distribution of BNNSs and BN-800-2 in *C. elegans* by fluorescence microscopy, rhodamine B (RhoB) was loaded by blending it (1 mg) with BNNSs (10 mg each) or BN-800-2 (10 mg each) in 5 mL Milli-Q water over 24 hours at 20°C away from light. Uncombined RhoB was eliminated by dialysis against Milli-Q water through a dialysis membrane (molecular weight cutoff=1,000) over 72 hours. The BNNSs/RhoB and BN-800-2/RhoB produced were lyophilized and reserved at 4°C. For the test of distribution, *C. elegans* were cultured in 500  $\mu$ L K medium with BNNSs/RhoB or BN-800-2/RhoB at a concentration of 500  $\mu$ g·mL<sup>-1</sup> from L4-stage larvae for 24 hours away from light. For defecation assays, *C. elegans* were treated with RhoB-labeled BNNSs/RhoB or BN-800-2/RhoB for 24 hours at a

concentration of  $500 \mu\text{g}\cdot\text{mL}^{-1}$ , then transferred and washed with pure K medium. Complete defecation was defined as no RhoB-labeled BN materials observed in the whole intestinal lumen of worms, the amount of which was recorded at 0, 15, and 30 minutes and 1, 3, 5, and 7 hours after washing. The examined *C. elegans* were observed using fluorescence microscopy at 550 nm excitation wavelength and 575 nm emission filter.

## Statistical analysis

To analyze differences among all the groups, data acquired from growth assays, reproduction assays, locomotion-behavior assays, reactive oxygen species (ROS) assays, qRT-PCR, and distribution assays were evaluated with Student's *t*-test for unpaired data. Data from life-span assays were calculated by Kaplan–Meier test. All statistical analyses were performed using SPSS 18.0 (SPSS Inc, Chicago, IL, US). Probability levels (*P*-values) of 0.05 or 0.01 were considered statistically significant.

## Results

### Characterization of BNNSs and BN-800-2

TEM imaging revealed that a single BNNS was 150 nm in diameter (Figure 1A). Because BN-800-2 showed poly-morphic lamellar structure (Figure 1B), we measured the maximum diameter of aggregations less than 700 nm, in agreement with previous reports.<sup>9,29</sup> Figure S1 shows that BN-800-2 displayed better solubility than BNNS suspensions in deionized water or K medium at a concentration of  $500 \mu\text{g}\cdot\text{mL}^{-1}$  after sonication for 10 minutes. The hydrodynamic size of BNNSs was nearly twice as large as BN-800-2 in deionized water or K medium after sonication (Table 1). It is possible that lower average surface charge and fewer hydrophilic surface groups (eg, –OH) make BNNSs easier to aggregate than BN-800-2 in solution.<sup>9,29</sup>

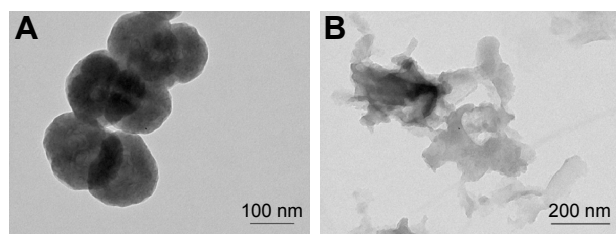


**Figure 1** TEM images of BNNSs and BN-800-2.

**Notes:** BNNSs (A) and BN-800-2 (B) in water after sonication.

**Abbreviations:** TEM, transmission electron microscopy; BNNSs, boron nitride nanospheres; BN-800-2, highly water-soluble boron nitride.

### Effects of life span of BNNSs or BN-800-2 on *C. elegans* life span

To investigate the effect of BN NMs on the life span of *C. elegans*, the animals were cultured with different concentrations of BNNSs or BN-800-2 from L4 larval developmental stage. Compared to the untreated control, the average life span was significantly reduced by approximately 3 days in the  $100 \mu\text{g}\cdot\text{mL}^{-1}$  and  $500 \mu\text{g}\cdot\text{mL}^{-1}$  BNNS-exposed group and 3 and 6 days in the  $100 \mu\text{g}\cdot\text{mL}^{-1}$  and  $500 \mu\text{g}\cdot\text{mL}^{-1}$  BN-800-2-exposed group, respectively (Figure 2A and B). These observations indicate that BN-800-2 shortened animal life span more significantly than BNNSs, likely due to its higher solubility.

### Effects of BNNSs or BN-800-2 on growth, locomotion behavior, and reproduction of *C. elegans*

To evaluate the developmental toxicity of BN NMs, the body size of *C. elegans* was first measured. BNNS exposure at all the concentrations tested did not affect body extension during the L1 larval stage through adulthood (72 hours) (Figure 2C), whereas BN-800-2 exposure significantly reduced body length at concentrations over  $100 \mu\text{g}\cdot\text{mL}^{-1}$  (Figure 2D). These observations indicate that BN-800-2 but not BNNSs impaired the growth of worms.

To investigate the behavioral influence of BN NMs, toxic tests for locomotion were performed on L4 larval *C. elegans* exposed to BN NMs for 24 hours. Both BNNS and BN-800-2 exposure ( $500 \mu\text{g}\cdot\text{mL}^{-1}$ ) resulted in a mild reduction in head-thrash behavior, with BN-800-2 causing slightly more severe defects (Figure 2E). Similarly, BN-800-2 significantly affected more body bending (19.87%, 30.05%, and 34.12% for 10, 100, and  $500 \mu\text{g}\cdot\text{mL}^{-1}$ , respectively) than BNNSs (6.62%, 12.46%, and 22.62% for 10, 100, and  $500 \mu\text{g}\cdot\text{mL}^{-1}$ , respectively; Figure 2F). Since locomotion is thought to be a sensitive indicator reflecting motor-neuron damage during ENM exposure,<sup>20,36,37</sup> we detected GFP-labeled *UNC47* gene (a transmembrane vesicular GABA transporter) to evaluate the function of D-type GABAergic motor neurons, which innervate the dorsal and ventral body muscles (Figure S2).<sup>38</sup> The decreased expression of *UNC47* in BNNS or BN-800-2 (90.77% and 88.39%, respectively) exposure suggests slight neurotoxicity induced by BN materials (Figure S2), consistent with the observed modest locomotion impairment (Figure 2E and F).

To examine the influence on reproductive organs, the number of progeny per worm was counted daily until



egg-laying stopped, which was often on day 11 postembryonically. Both BNNSs and BN-800-2 significantly decreased the number of progeny at concentrations of  $100 \mu\text{g}\cdot\text{mL}^{-1}$  and  $500 \mu\text{g}\cdot\text{mL}^{-1}$ . Of note, exposure to  $500 \mu\text{g}\cdot\text{mL}^{-1}$  BN-800-2

reduced reproductivity to approximately a third that of BNNSs (Figure 2G). These results collectively indicate that the highly water-soluble BN-800-2 is more toxic than hydrophobic BNNSs in growth, locomotion behavior, and reproduction.

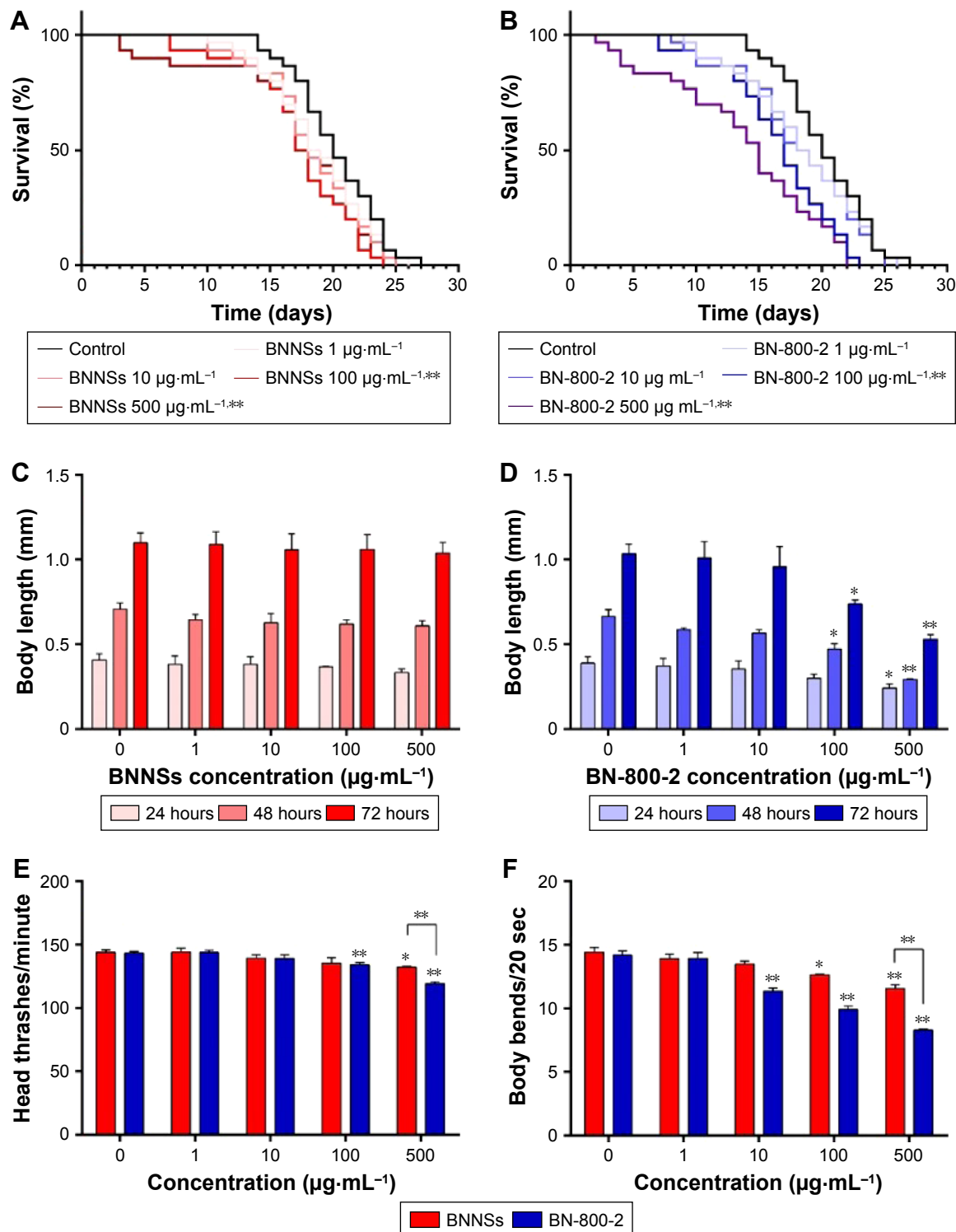
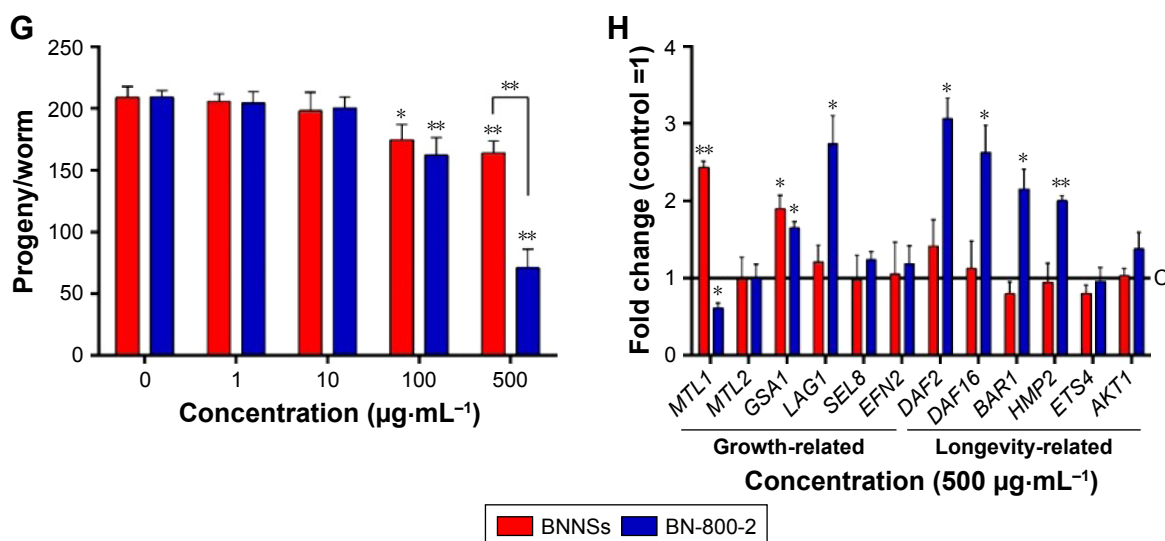


Figure 2 (Continued)



**Figure 2** Biological adverse effects of BNNSs and BN-800-2 on life span, growth, locomotion behavior, progeny, and expression of related genes in *Caenorhabditis elegans*. **Notes:** Adverse effect on the life span of age-synchronized L4-stage larvae exposed to different concentrations of BNNSs (A) or BN-800-2 (B), cultured consecutively (n=30). The length of *C. elegans* on exposure to different concentrations of BNNSs (C) or BN-800-2 (D) was measured every 24 hours from L1-stage larvae to adults for 3 days consecutively (n=10, three repeats). Effects of exposure to BNNSs or BN-800-2 on head thrashes (E) and body bends (F) of L4-stage larvae after exposure for 24 hours (n=15, three repeats). (G) Number of progeny per worm exposed successively to different concentrations of BNNSs or BN-800-2 in L4-stage larvae (n=10). (H) Relative expression of growth- and longevity-related genes in L4-stage larvae with exposure to BNNSs or BN-800-2 at a concentration of 500 µg·mL<sup>-1</sup> for 24 hours (n=3). Three experimental repeats (three technical replicates for each experiment); C, control. All genes were normalized to *ACT1* mRNA level and expressed as fold change relative to the untreated control. Worms were maintained in K medium in 24-well plates at 20°C in an incubator. Data presented as means ± SEM. \*P<0.05; \*\*P<0.01. **Abbreviations:** BNNSs, boron nitride nanospheres; BN-800-2, highly water-soluble boron nitride; SEM, standard error of mean.

## Expression of growth- and longevity-related genes in BNNS- or BN-800-2-exposed *C. elegans*

To investigate further the molecular basis of BN-material toxicity, six growth-related genes (*MTL1*, *MTL2*, *GSA1*, *LAG1*, *SEL8*, and *EFN2*) and six lifespan-related genes (*DAF2*, *DAF16*, *BAR1*, *HMP2*, *ETS4*, and *AKT1*) were examined in exposed worms (Table S1). BNNS exposure significantly increased the expression of two growth-related genes: *MTL1* (encoding metallothioneins) and *GSA1* (encoding the mammalian orthologue of heterotrimeric G protein) (Figure 2H). In contrast, BN-800-2 exposure increased the expression of two growth-related genes – *GSA1* and *LAG1* (encoding the orthologue of the CBF1–RBP–JK–SuH–LAG1 family) – and four lifespan-related genes: *DAF2* (encoding the orthologue of insulin/IGF receptor), *DAF16* (encoding the orthologue of FoxO), *BAR1*, and *HMP2* (encoding the orthologue of β-catenin) (Figure 2H). These data indicated that compared to BNNSs, BN-800-2 affected the expression of a wider spectrum of genes, consistent with BN-800-2's higher toxicity to growth and life span.

## Exposure to BNNSs and BN-800-2 causes oxidative stress in *C. elegans*

ROS-induced oxidative stress is thought partly to account for ENM toxicity.<sup>39</sup> To assess oxidative stress caused by BN

materials, we measured ROS levels in worms after treatment with BN materials for 24 hours (Figure 3A and B). While BNNSs increased ROS-fluorescence intensity at concentrations higher than 100 µg·mL<sup>-1</sup>, BN-800-2 promoted ROS generation at a lower concentration, 10 µg·mL<sup>-1</sup>, and effectively produced more ROS than BNNSs (2.7-fold for 100 µg·mL<sup>-1</sup> and 3.4-fold for 500 µg·mL<sup>-1</sup>) (Figure 3B). Given that ROS production indicates the toxicity of nanobiomaterials, eg, GO,<sup>28</sup> CNTs,<sup>26</sup> TiO<sub>2</sub>, and ZnO,<sup>36,40</sup> our data here suggest that ROS overproduction in the intestine tissue might be one of the mechanisms underlying adverse BNNS and BN-800-2 effects.

## Exposure to BNNSs and BN-800-2 affects the expression of oxidative stress-related genes

Several antioxidant genes, such as superoxide dismutases, catalases, and glutathione-S-transferase, regulate ROS-triggered damage by catalyzing the ROS-scavenging progress.<sup>41</sup> To examine the role of ROS in the toxicity of BNNSs and BN-800-2, 16 genes related to oxidative-stress response were investigated in exposed *C. elegans* (Table S1). Compared to the control group, the mRNA levels of 14 stress-response genes involved in oxygen metabolism were altered in *C. elegans* exposed to 500 µg·mL<sup>-1</sup> of BN-800-2. These genes were *HSP16.1*, *HSP4*, *HSP70*, *ISP1*, *SOD1*, *SOD2*, *SOD3*, *CTL2*, *GAS1*, *GCS1*, *GST4*, *CLK1*, *PMK1*, and *MEK1*

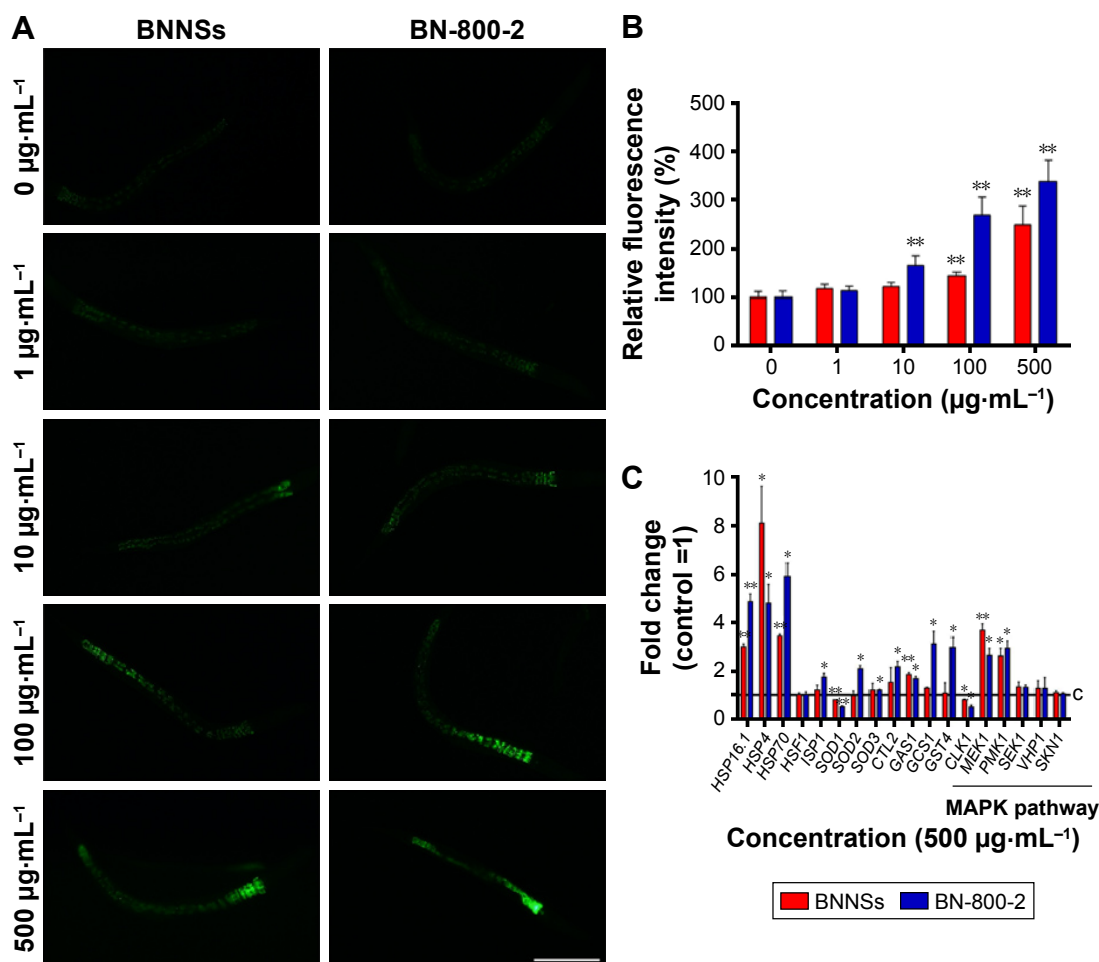


**Figure 3** Alterations in ROS production and related-gene mRNA levels in BNNSs- or BN-800-2-exposed *Caenorhabditis elegans*.

**Notes:** (A) Representative fluorescent micrograph showed intestinal ROS production in worms exposed to BNNSs or BN-800-2 at different concentrations for 24 hours. (B) Quantification of average integrated optical density of ROS production in BNNSs- or BN-800-2-exposed *C. elegans* (n=50). (C) Relative expression of genes related to oxidative stress response, including MAPK-signaling pathway, in *C. elegans* with exposure to BNNSs or BN-800-2 at a concentration of 500 µg·mL<sup>-1</sup>. Three experimental repeats (three technical replicates for each experiment); C, control. All the respective mRNA levels were normalized to *ACT1* mRNA levels and expressed as fold change relative to the untreated control. All experiments were done by exposing L4-stage larvae to BNNSs or BN-800-2 into K medium in 24-well plates for 24 hours at 20°C. Data presented as means ± SEM. \*P<0.05; \*\*P<0.01. Scale bar 200 µm.

**Abbreviations:** ROS, reactive oxygen species; BNNSs, boron nitride nanospheres; BN-800-2, highly water-soluble boron nitride; SEM, standard error of mean.

(Figure 3C). In contrast, the exposure of BNNSs changed the expression of fewer genes to a lesser extent (Figure 3C). These results indicate that BN-800-2 more prevalently affected the expression of ROS-related genes than BNNSs, suggesting BN-800-2 might induce more severe oxidative damage. Similarly, other ENM exposure also led to changed expression levels in oxidation-related genes, such as upregulation of *SOD2*, *SOD3*, *ISPI*, *GAS1*, and *CLK1* for CNT exposure,<sup>42</sup> upregulation of *SOD1*, *SOD2*, *SOD3*, *ISPI*, and *CLK1* for GO exposure,<sup>28</sup> and upregulation of *HSP16.1*, *HSP70*, *SOD1*, *SOD2*, *SOD3*, and *CTL2* for ZnO NP exposure.<sup>40</sup>

### Biodistribution of BNNSs and BN-800-2 in *C. elegans*

Previous research revealed that the translocation level of ENMs from the primarily targeted organs in *C. elegans*

(such as the epithelial cells of the intestine) to the secondarily targeted organs (such as alimentary and reproductive organs) was positively correlated with ENM toxicity.<sup>20,43</sup> To test whether this was also the case for BN materials, BNNSs and BN-800-2 were visualized by RhoB labeling in treated worms. After exposure for 24 hours, most BNNSs or BN-800-2 were distributed within the primarily targeted organs (pharynx and digestive tract), with a small amount translocated to the head regions outside the pharynx (Figure 4A, C, and D). Approximately half of BNNSs/RhoB and BN-800-2/RhoB were retained in the body after 24-hour defecation (Figure 4B–D) and totally defecated from the intestinal lumen within 7 hours (Figure S3), suggesting that the worms did not have biological preferences on the translocation, accumulation, or excretion of BNNSs and BN-800-2. To locate more precisely the distribution sites of BNNSs

and BN-800-2, we used a transgenic strain of *AJM1-jcIs1*. This strain expresses GFP-fused AJM1 protein, an apical junction molecule of cells localized in intestine, pharynx, and vulva.<sup>44</sup> BNNSs and BN-800-2 remained mainly in primarily targeted organs, but not in secondarily targeted organs, such

as the gonad and embryos, suggesting that the observed secondarily targeted organ-related functional defects caused by BN material exposure, including locomotion-behavior defects and progeny reduction, might have been induced by indirect effects, possibly ROS production (Figure 5).

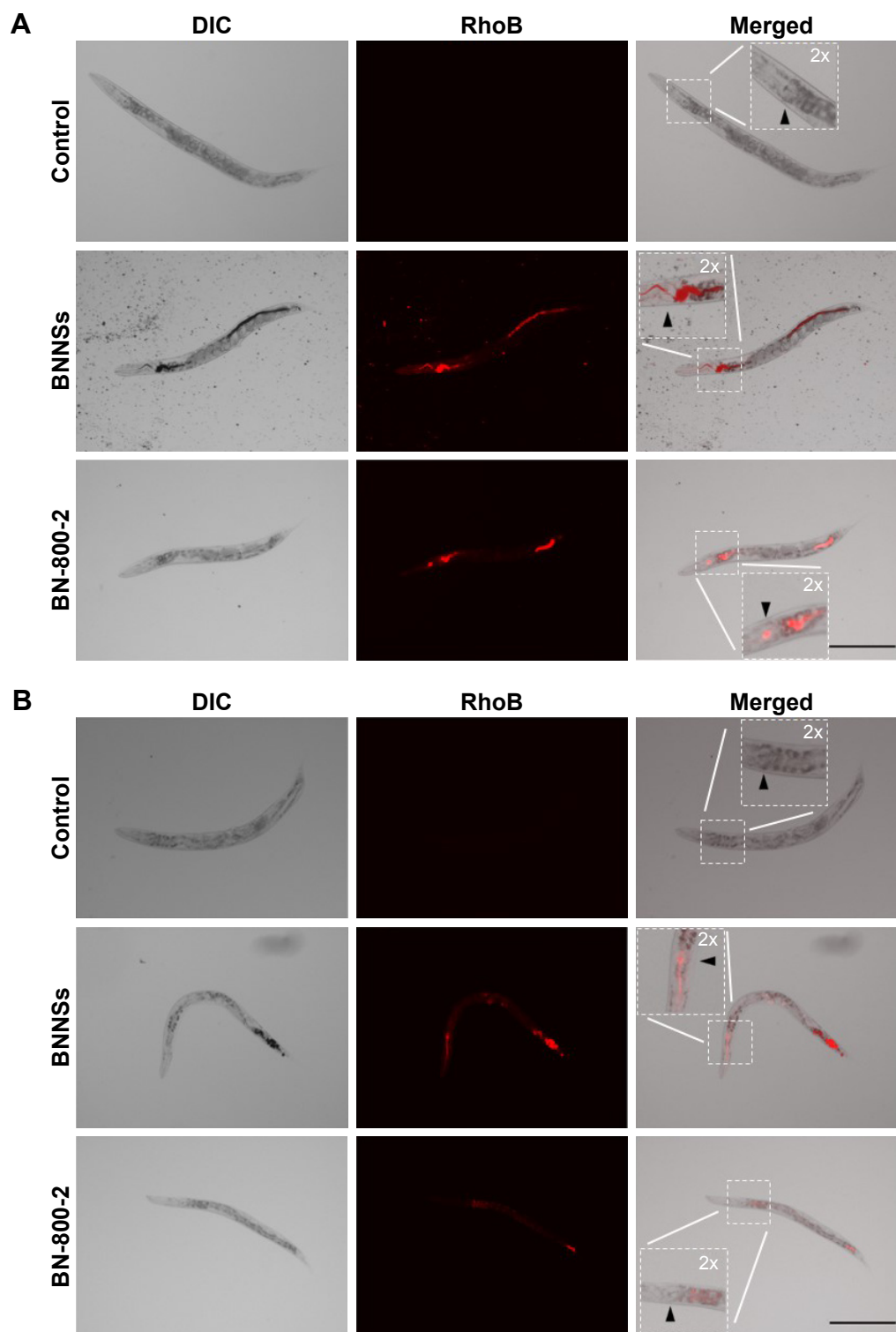
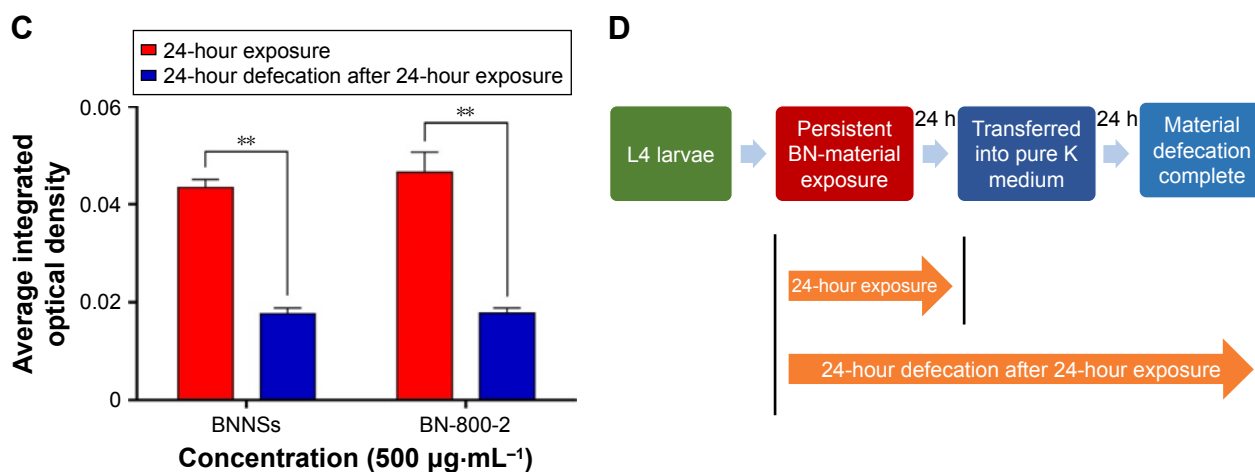


Figure 4 (Continued)





**Figure 4** In vivo accumulation of BNNSs or BN-800-2 in *Caenorhabditis elegans*.

**Notes:** (A) Representative fluorescent micrograph of control (untreated) and L4-stage larvae after being treated with RhoB-labeled BNNSs or BN-800-2 (500  $\mu\text{g}\cdot\text{mL}^{-1}$ ) for 24 hours. Arrowheads indicate the pharynx. Inset images are enlargements of regions outlined by small boxes. (B) After being treated as in A, worms were transferred and cultured in pure K medium for defecation for 24 hours. (C) Quantification of average integrated optical density of RhoB in worms with persistent 24-hour exposure or worm-defecated materials for 24 hours after being treated as in A (n=50). (D) In vivo accumulation-assay procedure for exposure and defecation of BN materials. Worms were maintained in K medium in 24-well plates at 20°C in an incubator. Data presented as means  $\pm$  SEM. \*\*P<0.01. Scale bar 200  $\mu\text{m}$ .

**Abbreviations:** BN, boron nitride; BNNSs, boron nitride nanospheres; BN-800-2, highly water-soluble boron nitride; DIC, differential interference contrast; RhoB, rhodamine B; SEM, standard error of mean.

## ROS production and BN accumulation in BNNS- or BN-800-2-exposed wild-type and mutant strains

Oxidative stress-related genes play important roles in ROS-induced toxicity for some ENMs, such as GO, TiO<sub>2</sub> NPs and Al<sub>2</sub>O<sub>3</sub> NPs.<sup>24,36,37</sup> To determine whether these genes were also involved in the toxicity induced by BN materials, we assessed the ROS production in wild-type and five mutant strains of oxygen-metabolism genes (*GAS1*, *SOD2*,

and *SOD3*) and MAPK-signaling genes (*MEK1* and *PMK1*) required for oxidative stress responses in L4 larvae exposed to BNNSs or BN-800-2 (500  $\mu\text{g}\cdot\text{mL}^{-1}$ ). Previous studies have demonstrated that defects in *GAS1*, *SOD2*, *SOD3*, *MEK1*, and *PMK1* can increase ROS levels and enhance oxidative cellular damage.<sup>45–47</sup> Our results showed that exposure to either BNNSs or BN-800-2 elevated ROS production in *GAS1*, *SOD2*, *SOD3*, and *MEK1* mutants, suggesting the suppressive functional roles of *GAS1*, *SOD2*, *SOD3*, and *MEK1* genes in ROS production (Figure 6). Interestingly, the *PMK1* mutant

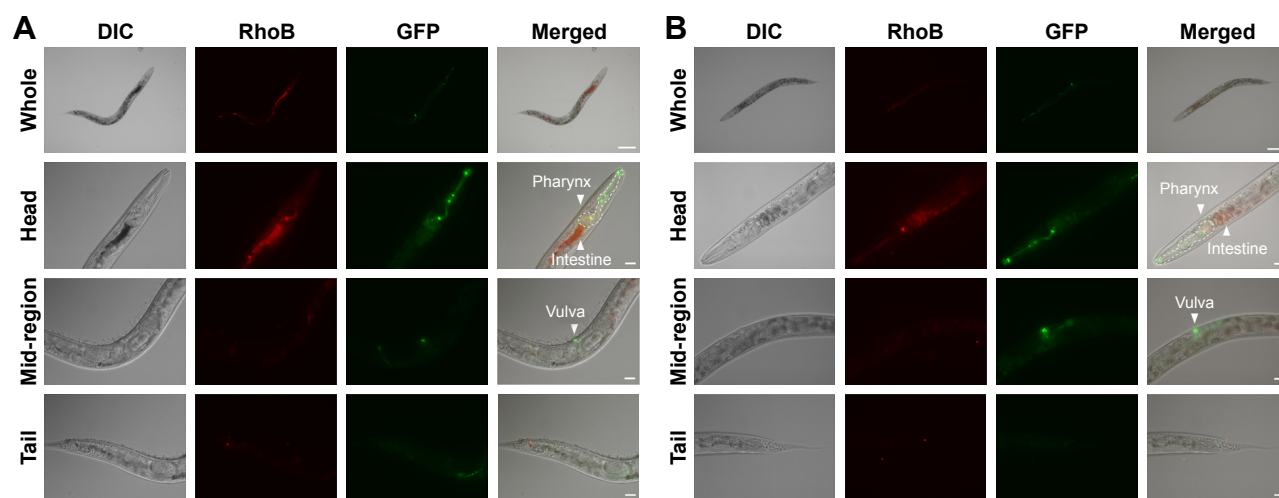


**Figure 5** In vivo distribution of BNNSs and BN-800-2 in transgenic strain of AJM1.

**Notes:** Representative fluorescent micrograph of L4-stage larvae treated with (A) RhoB-labeled BNNSs (500  $\mu\text{g}\cdot\text{mL}^{-1}$ ) or (B) BN-800-2 (500  $\mu\text{g}\cdot\text{mL}^{-1}$ ) in K medium for 24 hours (n=50). GFP labels mouth, pharynx, vulva, and part of intestine. Scale bars 100  $\mu\text{m}$  and 20  $\mu\text{m}$ , respectively.

**Abbreviations:** BNNSs, boron nitride nanospheres; BN-800-2, highly water-soluble boron nitride; DIC, differential interference contrast; RhoB, rhodamine B.

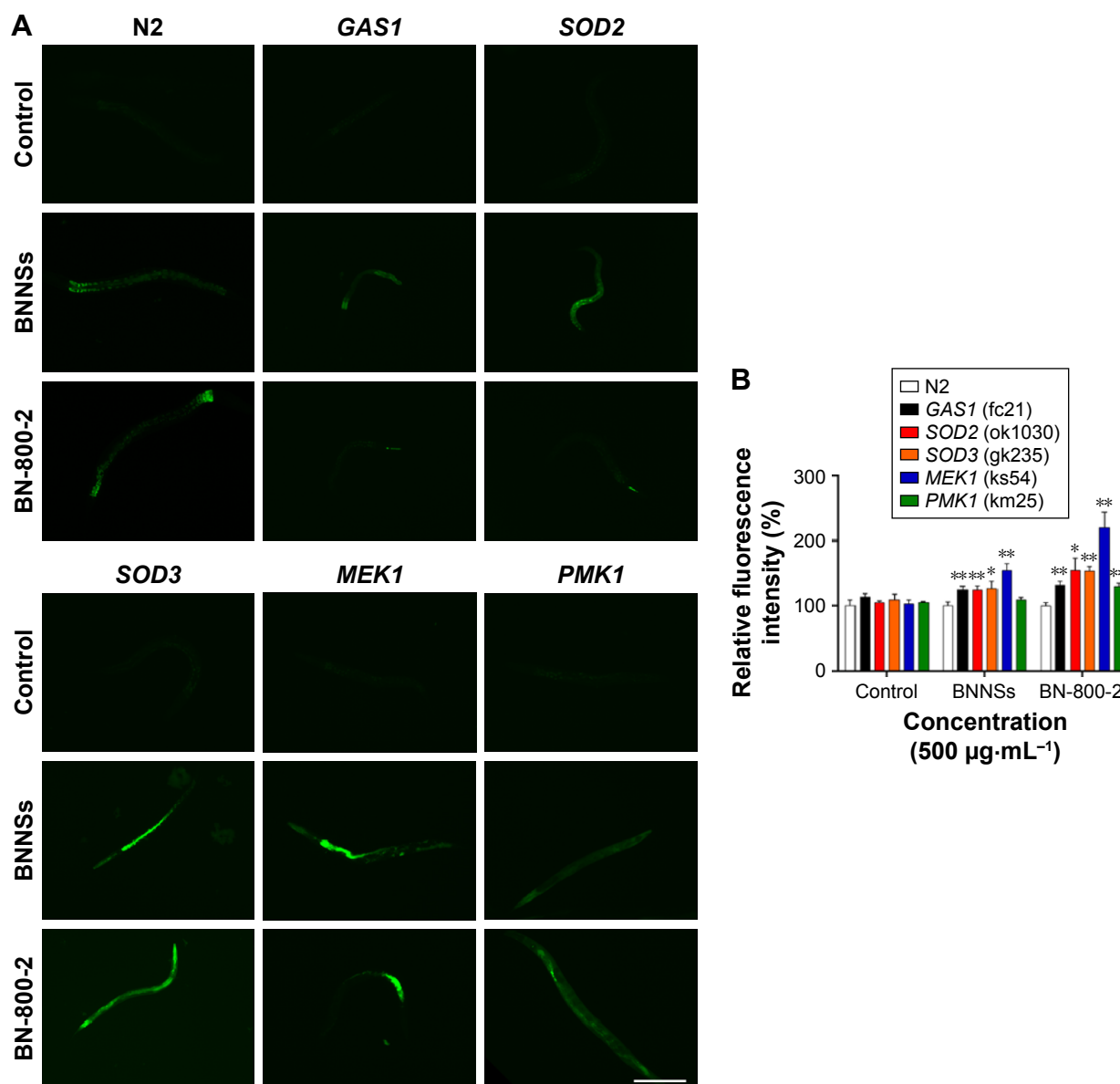


**Figure 6** ROS production in BNNS- and BN-800-2-exposed wild-type and mutant worms.

**Notes:** (A) Representative fluorescent micrographs show intestinal ROS production in the wild-type and five mutants treated with BNNSs or BN-800-2 at a concentration of 500  $\mu\text{g}\cdot\text{mL}^{-1}$ . (B) Quantification of average integrated optical density of ROS visualized by ROS probe in the mutants indicated in A (n=50). The wild-type and five mutant worms at L4-stage larvae were treated with indicated BN materials in K medium for 24 hours. Data presented as means  $\pm$  SEM, \* $P$ <0.05; \*\* $P$ <0.01. Scale bar 200  $\mu\text{m}$ .

**Abbreviations:** ROS, reactive oxygen species; BNNSs, boron nitride nanospheres; BN-800-2, highly water-soluble boron nitride; SEM, standard error of mean.

produced more ROS than the wild type only when exposed to BN-800-2. Considering that *PMK1* enhances the activities of SOD and catalase,<sup>48</sup> these data suggest the MAPK-signaling pathway may be needed for eliminating ROS production induced specifically by BN-800-2.

We next determined whether the accumulation of BNNSs and BN-800-2 was influenced by ROS. The accumulation of BNNSs or BN-800-2 was significantly increased in *SOD2*, *SOD3*, and *MEK1* mutants than in the wild type, suggesting that Mn-SODs and the MAPK-signaling pathway inhibit the accumulation of BNNSs and BN-800-2 (Figure 7), consistent with the role of these genes in regulating the accumulation of

other ENMs.<sup>37,42</sup> Given the known functional role of *SOD2* and *SOD3* in scavenging ROS, *SOD2* and *SOD3* inhibition of BN accumulation was likely due to reduced ROS production, suggesting that ROS might be involved in promoting BN-material in vivo accumulation.

### Effects of BNNSs and BN-800-2 on growth and locomotion behavior in wild types and mutants

*MEK1* encodes a homologue of mammalian MKK7 and promotes growth and movement in the presence of heavy metals and starvation.<sup>49</sup> In *MEK1* mutants, a 72-hour exposure to

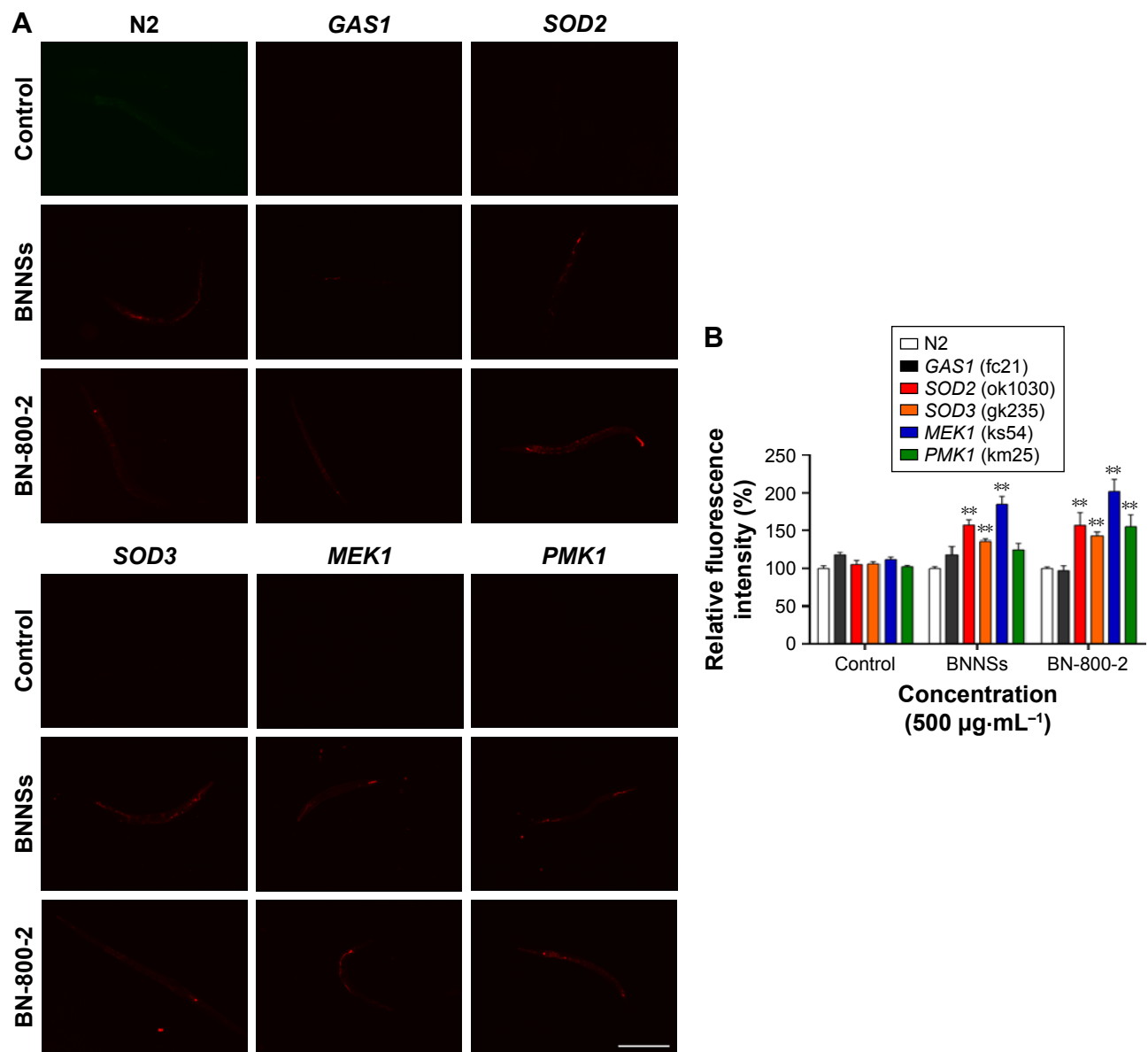


**Figure 7** BN-material accumulation in wild-type and mutant worms.

**Notes:** (A) Representative fluorescent micrograph of indicated mutants treated with RhoB-labeled BNNSs and BN-800-2 ( $500 \mu\text{g}\cdot\text{mL}^{-1}$ ). The control was untreated. (B) Quantification of average integrated optical density of RhoB in worms from A ( $n=50$ ). Wild-type and five mutant worms at L4 larval stage were treated with indicated BN materials in K medium for 24 hours. Data presented as means  $\pm$  SEM.  $**P<0.01$ . Scale bar  $200 \mu\text{m}$ .

**Abbreviations:** BNNSs, boron nitride nanospheres; BN-800-2, highly water-soluble boron nitride; RhoB, rhodamine B; SEM, standard error of mean.

BN-800-2 significantly shortened body length in comparison to the wild type (Figure 8A), suggesting that the increased ROS production caused by BN-800-2 exposure likely accounted for retarded growth. Further, the locomotion defects in head thrashes and body bends were also observed in *MEK1* and *GAS1*, *SOD2*, and *SOD3* mutants, whose corresponding genes are all involved in oxidative stress regulation (Figure 8B and C). Given that locomotion is a sensitive indicator reflecting neuronal damage during ENM exposure, these results suggest that these genes may suppress neuronal damage, possibly through their effects in reducing ROS. We next investigated the effects of *MEK1* or *PMK1* mutation

for mRNA transcription of stress-response genes in BNNS and BN-800-2 ( $500 \mu\text{g}\cdot\text{mL}^{-1}$ )-exposed worms. Figure S4 shows mutant *MEK1* or *PMK1* inhibited the upregulation of *MTL1* with exposure to BNNSs. Mutant *MEK1* inhibited the upregulation of *GCSI*, and mutant *PMK1* inhibited both *GCSI* and *GST4* with exposure to BNNSs and BN-800-2, respectively (Figure S4).

## Discussion

The toxicity of ENMs is thought to be positively correlated with their solubility.<sup>50,51</sup> For instance, the toxic threshold for soluble GO is lower than hydrophobic graphene in *C. elegans*

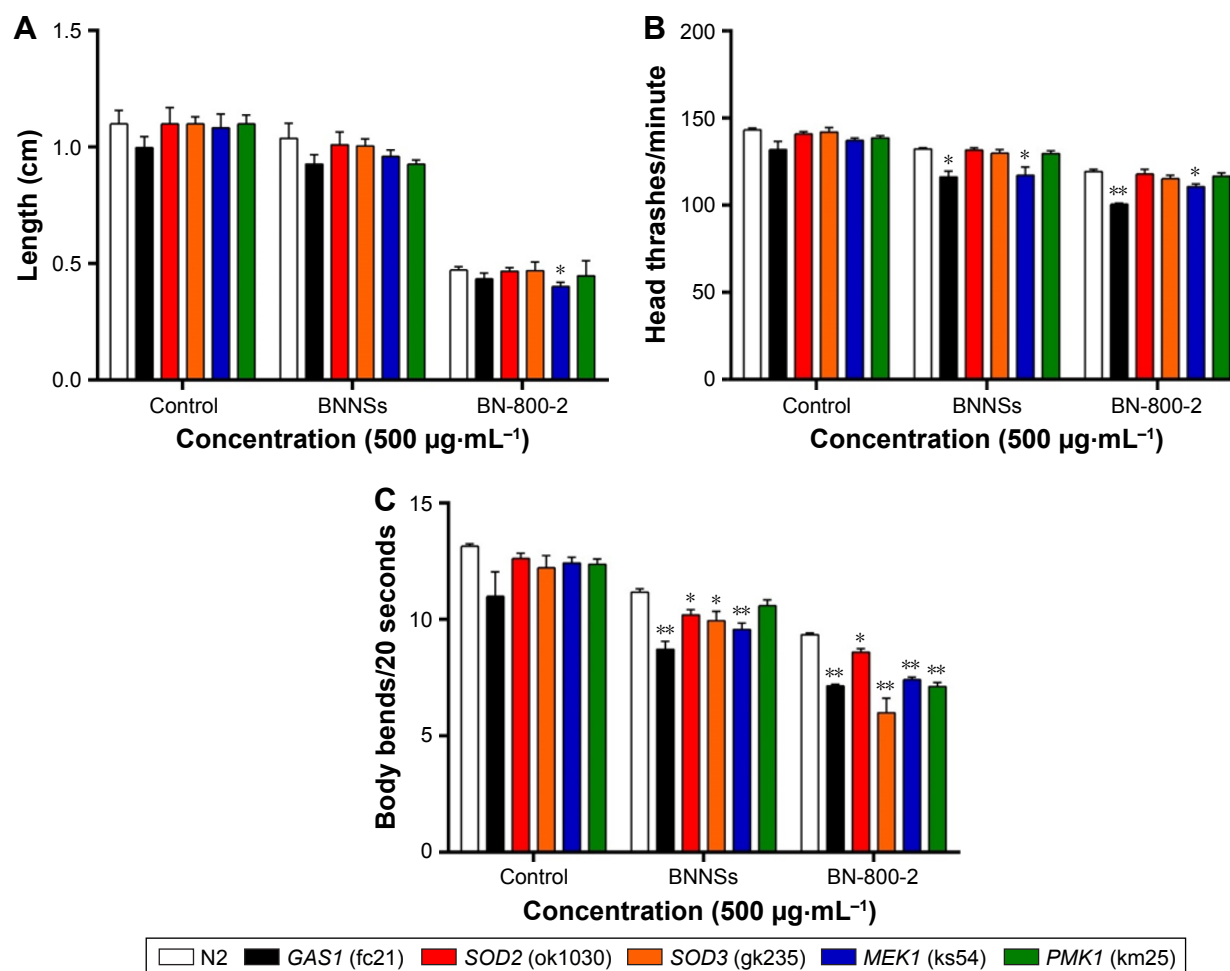


**Figure 8** Growth and locomotion defects in BN-exposed mutants.

**Notes:** (A) Length of wild-type and mutant larvae consecutively exposed to 500  $\mu\text{g}\cdot\text{mL}^{-1}$  of BNNSs or BN-800-2 from L1-stage larvae was measured every 24 hours for 3 days ( $n=10$ , three repeats). Effects of exposure to BNNSs or BN-800-2 on head thrashes (B) and body bends (C) in wild-type and mutant L4-stage larvae after exposure for 24 hours ( $n=15$ , three repeats). Worms were maintained in K medium in 24-well plates at 20°C. Data presented as means  $\pm$  SEM. \* $P<0.05$ ; \*\* $P<0.01$ .

**Abbreviations:** BNNSs, boron nitride nanospheres; BN-800-2, highly water-soluble boron nitride; SEM, standard error of mean.

(10  $\mu\text{g}\cdot\text{mL}^{-1}$  vs >50  $\mu\text{g}\cdot\text{mL}^{-1}$ ).<sup>21,28</sup> Moreover, for metal NPs in *C. elegans*, the toxic threshold of highly soluble  $\text{Al}_2\text{O}_3$  NPs and ZnO NPs is lower than bulk  $\text{Al}_2\text{O}_3$  (8.1  $\mu\text{g}\cdot\text{mL}^{-1}$  vs 23.1  $\mu\text{g}\cdot\text{mL}^{-1}$ )<sup>24</sup> and ZnO (0.45  $\mu\text{g}\cdot\text{mL}^{-1}$  vs 2.25  $\mu\text{g}\cdot\text{mL}^{-1}$ ).<sup>40</sup> Similarly, our data demonstrate that the threshold for the highly water-soluble BN-800-2 to cause locomotion defects and ROS production was significantly lower than that for BNNSs (10  $\mu\text{g}\cdot\text{mL}^{-1}$  vs 100  $\mu\text{g}\cdot\text{mL}^{-1}$ ). Importantly, compared to carbon or metal NPs, the toxicity of BNNSs and BN-800-2 was lower in *C. elegans*, suggesting relatively good biocompatibility.

Although the accumulated amount of BN-800-2 and BNNSs within primary-target organs was similar, our results showed that soluble BN-800-2 induced more ROS production than BNNSs, suggesting that BN-800-2 is more toxic than BNNSs. Consistently, BN-800-2 exposure promoted more ROS production than BNNS exposure in most of the

loss-of-function mutants of the key antioxidative genes. Given that ROS can impair biological barrier integrity, such as the intestinal epithelium, the observation that increased ROS production was correlated with enhanced BN-material in vivo accumulation might suggest a positive feedback between ROS production and the amount of BN retained in primarily targeted organs. Oxidative stress induced by ROS underlies the toxicity of ENMs, including behavior dysfunction and development.<sup>40,42</sup> Supporting this notion, BN-800-2 exposure that produced more ROS than BNNS exposure consistently resulted in more severe defects in locomotion behavior (head thrashes/body bending) and postembryonic growth (body length) in the antioxidative mutants. Such locomotion defects are thought to be due to ROS neurotoxicity.<sup>24</sup> Our data showed that mitochondrial complex I, Mn-SOD, and MAPK signaling (*GAS1*, *SOD2*, *SOD3*, and *MEK1* genes) were responsible for reducing BN



material-induced ROS generation, which possibly in turn suppressed neurotoxicity.

Interestingly, while *GAS1*, *SOD2*, *SOD3*, and *MEK1* were four shared genes associated with the toxicity of both BNNSs and BN-800-2, *PMK1* appeared to be specifically required to suppress the multiple aspects of BN-800-2 toxicity. This observation indicates the involvement of *PMK1* in antioxidative responses to BN-800-2 exposure, reflecting that BNNSs and BN-800-2 are capable of activating different antioxidative pathways, which might also contribute to the differences in toxicity observed between BNNSs and BN-800-2. Our results also implied that *PMK1* might regulate BN-800-2 toxicity and accumulation through the transcriptional expression of *GCSI* and *GST4* (Figure S4) which are required for the synthesis of anti-ROS production of the polypeptide glutathione in *C. elegans*.

## Conclusion

Our comprehensive data from an in vivo whole-animal model indicate that BNNS biocompatibility was higher than BN-800-2. High-dose exposure of BN-800-2 (over  $10 \mu\text{g}\cdot\text{mL}^{-1}$ ) caused multiple functional defects in *C. elegans*. The oxidative damage induced by ROS played an important role in the toxicity of BNNSs and BN-800-2, and was regulated by oxidative-stress response and MAPK-signaling-related genes, such as *GAS1*, *SOD2*, *SOD3*, *MEK1*, and *PMK1*.

## Acknowledgments

NW and HW contributed equally to this work. This work was supported by National Natural Science Foundation of China Programs (81272559, 81402875, and 81572866), the International Science and Technology Corporation Program of the Chinese Ministry of Science and Technology (S2014ZR0340), and the Science and Technology Program of the Chinese Ministry of Education (113044A), the Frontier Exploration Program of Huazhong University of Science and Technology (2015TS153), the Natural Science Foundation Program of Hubei Province (2015CFA049), and the Hubei Province Hundreds of Talents Program.

## Disclosure

The authors report no conflicts of interest in this work.

## References

- Conde J, Dias JT, Grazú V, Moros M, Baptista PV, de la Fuente JM. Revisiting 30 years of biofunctionalization and surface chemistry of inorganic nanoparticles for nanomedicine. *Front Chem*. 2014;2:48.
- Song L, Ci L, Lu H, et al. Large scale growth and characterization of atomic hexagonal boron nitride layers. *Nano Lett*. 2010;10(8):3209–3215.
- Chen X, Wu P, Rousseas M, et al. Boron nitride nanotubes are non-cytotoxic and can be functionalized for interaction with proteins and cells. *J Am Chem Soc*. 2009;131(3):890–891.
- Peng J, Wang S, Zhang PH, Jiang LP, Shi JJ, Zhu JJ. Fabrication of graphene quantum dots and hexagonal boron nitride nanocomposites for fluorescent cell imaging. *J Biomed Nanotechnol*. 2013;9(10):1679–1685.
- Parra C, Montero-Silva F, Henriquez R, et al. Suppressing bacterial interaction with copper surfaces through graphene and hexagonal-boron nitride coatings. *ACS Appl Mater Interfaces*. 2015;7(12):6430–6437.
- Zhi C, Meng W, Yamazaki T, et al. BN nanospheres as CpG ODN carriers for activation of Toll-like receptor 9. *J Mater Chem*. 2011;21(14):5219–5222.
- Zhang H, Yamazaki T, Zhi C, Hanagata N. Identification of a boron nitride nanosphere-binding peptide for the intracellular delivery of CpG oligodeoxynucleotides. *Nanoscale*. 2012;4(20):6343–6350.
- Zhang H, Chen S, Zhi C, Yamazaki T, Hanagata N. Chitosan-coated boron nitride nanospheres enhance delivery of CpG oligodeoxynucleotides and induction of cytokines. *Int J Nanomedicine*. 2013;8:1783–1793.
- Weng Q, Wang B, Wang X, et al. Highly water-soluble, porous, and biocompatible boron nitrides for anticancer drug delivery. *ACS Nano*. 2014;8(6):6123–6130.
- Horváth L, Magrez A, Golberg D, et al. In vitro investigation of the cellular toxicity of boron nitride nanotubes. *ACS Nano*. 2011;5(5):3800–3810.
- Weng QH, Wang XB, Wang X, Bando Y, Golberg D. Functionalized hexagonal boron nitride nanomaterials: emerging properties and applications. *Chem Soc Rev*. 2016;45(14):3989–4012.
- Liu B, Qi W, Tian L, et al. In vivo biodistribution and toxicity of highly soluble peg-coated boron nitride in mice. *Nanoscale Res Lett*. 2015;10(1):478.
- Salveti A, Rossi L, Iacopetti P, et al. In vivo biocompatibility of boron nitride nanotubes: effects on stem cell biology and tissue regeneration in planarians. *Nanomedicine (Lond)*. 2015;10(12):1911–1922.
- Brenner S. The genetics of *Caenorhabditis elegans*. *Genetics*. 1974;77(1):71–94.
- Kaletta T, Hengartner MO. Finding function in novel targets: *C. elegans* as a model organism. *Nat Rev Drug Discov*. 2006;5(5):387–398.
- Boyd WA, McBride SJ, Freedman JH. Effects of genetic mutations and chemical exposures on *Caenorhabditis elegans* feeding: evaluation of a novel, high-throughput screening assay. *PLoS One*. 2007;2(12):e1259.
- Leung MC, Williams PL, Benedetto A, et al. *Caenorhabditis elegans*: an emerging model in biomedical and environmental toxicology. *Toxicol Sci*. 2008;106(1):5–28.
- Giacomotto J, Ségalat L. High-throughput screening and small animal models, where are we? *Br J Pharmacol*. 2010;160(2):204–216.
- Nel A, Xia T, Meng H, et al. Nanomaterial toxicity testing in the 21st century: use of a predictive toxicological approach and high-throughput screening. *Acc Chem Res*. 2013;46(3):607–621.
- Zhao Y, Wu Q, Lia Y, Wang D. Translocation, transfer, and in vivo safety evaluation of engineered nanomaterials in the non-mammalian alternative toxicity assay model of nematode *Caenorhabditis elegans*. *RSC Adv*. 2013;3(17):5741–5757.
- Jung SK, Qu X, Aleman-Meza B, et al. Multi-endpoint, high-throughput study of nanomaterial toxicity in *Caenorhabditis elegans*. *Environ Sci Technol*. 2015;49(4):2477–2485.
- Khare P, Sonane M, Pandey R, Ali S, Gupta KC, Satish A. Adverse effects of TiO<sub>2</sub> and ZnO nanoparticles in soil nematode, *Caenorhabditis elegans*. *J Biomed Nanotechnol*. 2011;7(1):116–117.
- Li Y, Wang W, Wu Q, et al. Molecular control of TiO<sub>2</sub>-NPs toxicity formation at predicted environmental relevant concentrations by Mn-SODs proteins. *PLoS One*. 2012;7(9):e44688.
- Li Y, Yu S, Wu Q, Tang M, Pu Y, Wang D. Chronic Al<sub>2</sub>O<sub>3</sub>-nanoparticle exposure causes neurotoxic effects on locomotion behaviors by inducing severe ROS production and disruption of ROS defense mechanisms in nematode *Caenorhabditis elegans*. *J Hazard Mater*. 2012;219–220, 221–230.

25. Zanni E, De Bellis G, Bracciale MP, et al. Graphite nanoplatelets and *Caenorhabditis elegans*: insights from an in vivo model. *Nano Lett*. 2012;12(6):2740–2744.
26. Chen PH, Hsiao KM, Chou CC. Molecular characterization of toxicity mechanism of single-walled carbon nanotubes. *Biomaterials*. 2013;34(22):5661–5669.
27. Nouara A, Wu Q, Li Y, et al. Carboxylic acid functionalization prevents the translocation of multi-walled carbon nanotubes at predicted environmentally relevant concentrations into targeted organs of nematode *Caenorhabditis elegans*. *Nanoscale*. 2013;5(13):6088–6096.
28. Wu Q, Yin L, Li X, Tang M, Zhang T, Wang D. Contributions of altered permeability of intestinal barrier and defecation behavior to toxicity formation from graphene oxide in nematode *Caenorhabditis elegans*. *Nanoscale*. 2013;5(20):9934–9943.
29. Tang C, Bando Y, Huang Y, Zhi C, Golberg D. Synthetic routes and formation mechanisms of spherical boron nitride nanoparticles. *Adv Funct Mater*. 2008;18(22):3653–3661.
30. Donkin SG, Williams PL. Influence of developmental stage, salts and food presence on various end points using *Caenorhabditis elegans* for aquatic toxicity testing. *Environ Toxicol Chem*. 1995;14(12):2139–2147.
31. Williams PL, Dusenbery DB. Aquatic toxicity testing using the nematode *Caenorhabditis elegans*. *Environ Toxicol Chem*. 1990;9(10):1285–1290.
32. Middendorf PJ, Dusenbery DB. Fluoroacetic acid is a potent and specific inhibitor of reproduction in the nematode *Caenorhabditis elegans*. *J Nematol*. 1993;25(4):573–577.
33. Tsalik EL, Hobert O. Functional mapping of neurons that control locomotory behavior in *Caenorhabditis elegans*. *J Neurobiol*. 2003;56(2):178–197.
34. Wang D, Shen L, Wang Y. The phenotypic and behavioral defects can be transferred from zinc-exposed nematodes to their progeny. *Environ Toxicol Pharmacol*. 2007;24(3):223–230.
35. Pfaffl MW. A new mathematical model for relative quantification in real-time RT-PCR. *Nucleic Acids Res*. 2001;29(9):e45.
36. Wu Q, Zhao Y, Li Y, Wang D. Susceptible genes regulate the adverse effects of TiO<sub>2</sub>-NPs at predicted environmental relevant concentrations on nematode *Caenorhabditis elegans*. *Nanomedicine*. 2014;10(6):1263–1271.
37. Wu Q, Zhao Y, Li Y, Wang D. Molecular signals regulating translocation and toxicity of graphene oxide in the nematode *Caenorhabditis elegans*. *Nanoscale*. 2014;6(19):11204–11212.
38. McIntire SL, Reimer RJ, Schuske K, Edwards RH, Jorgensen EM. Identification and characterization of the vesicular GABA transporter. *Nature*. 1997;389(6653):870–876.
39. Nel A, Xia T, Mädler L, Li N. Toxic potential of materials at the nano-level. *Science*. 2006;311(5761):622–627.
40. Khare P, Sonane M, Nagar Y, et al. Size dependent toxicity of zinc oxide nanoparticles in soil nematode *Caenorhabditis elegans*. *Nanotoxicology*. 2015;9(4):423–432.
41. Blokhina O, Virolainen E, Fagerstedt KV. Antioxidants, oxidative damage and oxygen deprivation stress: a review. *Ann Bot*. 2003;91(2):179–194.
42. Wu Q, Li Y, Li Y, et al. Crucial role of the biological barrier at the primary targeted organs in controlling the translocation and toxicity of multi-walled carbon nanotubes in the nematode *Caenorhabditis elegans*. *Nanoscale*. 2013;5(22):11166–11178.
43. Pluskota A, Horzowski E, Bossinger O, von Mikecz A. In *Caenorhabditis elegans* nanoparticle-bio-interactions become transparent: silica-nanoparticles induce reproductive senescence. *PLoS One*. 2009;4(8):e6622.
44. Köppen M, Simske JS, Sims PA, et al. Cooperative regulation of AJM-1 controls junctional integrity in *Caenorhabditis elegans* epithelia. *Nat Cell Biol*. 2001;3(11):983–991.
45. Kayser EB, Morgan PG, Sedensky MM. Mitochondrial complex I function affects haloethane sensitivity in *Caenorhabditis elegans*. *Anesthesiology*. 2004;101(2):365–372.
46. Neumann-Haefelin E, Qi W, Finkbeiner E, Walz G, Baumeister R, Hertweck M. SHC-1/p52Shc targets the insulin/IGF-1 and JNK signaling pathways to modulate life span and stress response in *C. elegans*. *Genes Dev*. 2008;22(19):2721–2735.
47. Suthamarak W, Somerlot BH, Opheim E, Sedensky M, Morgan PG. Novel interactions between mitochondrial superoxide dismutases and the electron transport chain. *Aging Cell*. 2013;12(6):1132–1140.
48. Zarse K, Schmeisser S, Groth M, et al. Impaired insulin/IGF1 signaling extends life span by promoting mitochondrial L-proline catabolism to induce a transient ROS signal. *Cell Metab*. 2012;15(4):451–465.
49. Koga M, Zwaal R, Guan KL, Avery L, Ohshima Y. A *Caenorhabditis elegans* MAP kinase kinase, MEK-1, is involved in stress responses. *EMBO J*. 2000;19(19):5148–5156.
50. Sun J, Wang F, Sui Y, et al. Effect of particle size on solubility, dissolution rate, and oral bioavailability: evaluation using coenzyme Q<sub>10</sub> as naked nanocrystals. *Int J Nanomedicine*. 2012;7:5733–5744.
51. Katsumiti A, Arostegui I, Oron M, Gilliland D, Valsami-Jones E, Cajaraville MP. Cytotoxicity of Au, ZnO and SiO<sub>2</sub> NPs using in vitro assays with mussel hemocytes and gill cells: relevance of size, shape and additives. *Nanotoxicology*. 2016;10(2):185–193.

## Supplementary materials

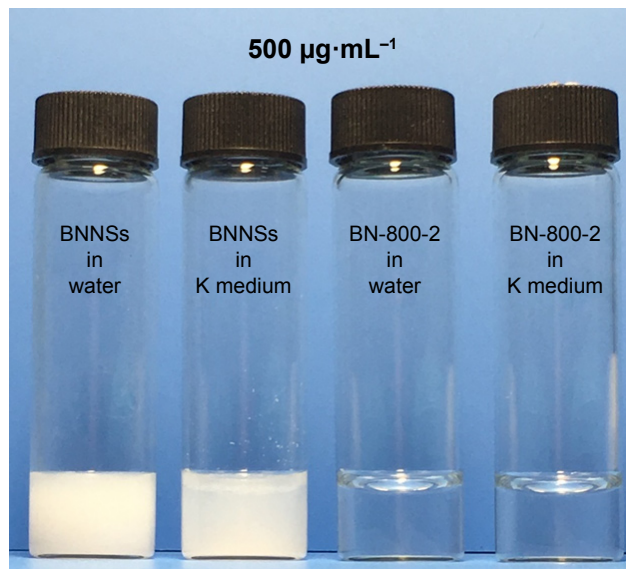


**Figure S1** BNNSs and BN-800-2 suspensions/solutions in water or K medium at a concentration of  $500 \mu\text{g}\cdot\text{mL}^{-1}$ .

**Notes:** BNNSs or BN-800-2 were suspended or dissolved into water or K medium, and the mixture was sonicated for 10 minutes.

**Abbreviations:** BNNSs, boron nitride nanospheres; BN-800-2, highly water-soluble boron nitride.

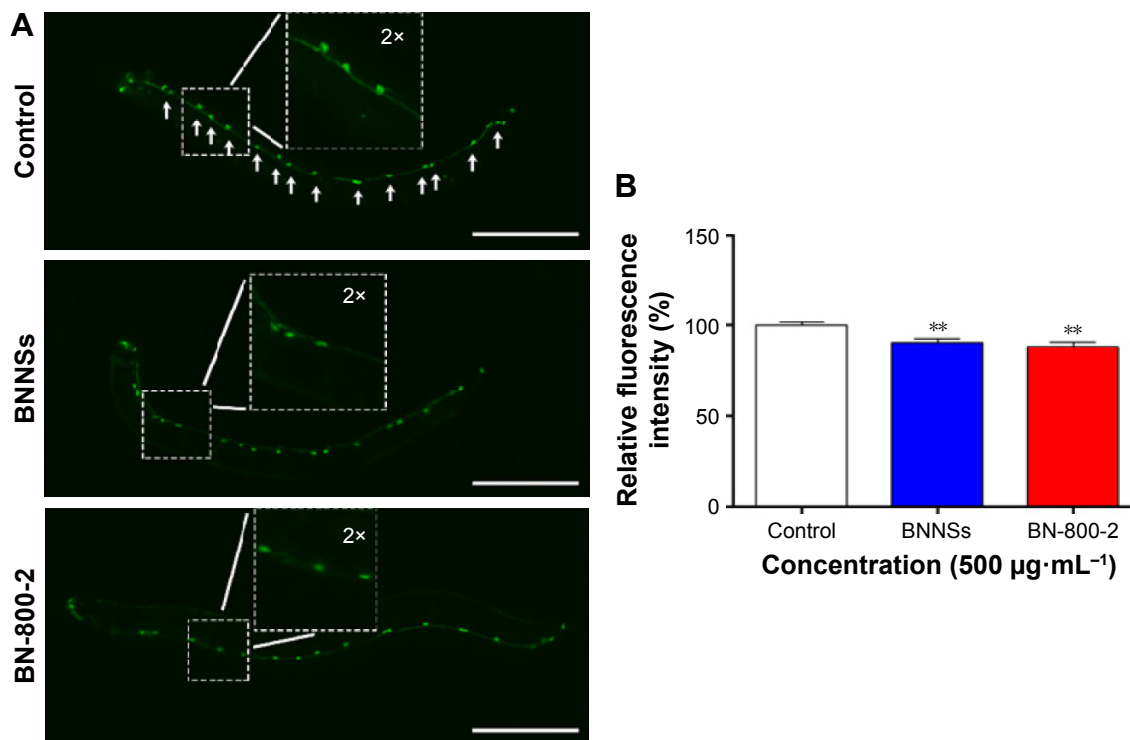


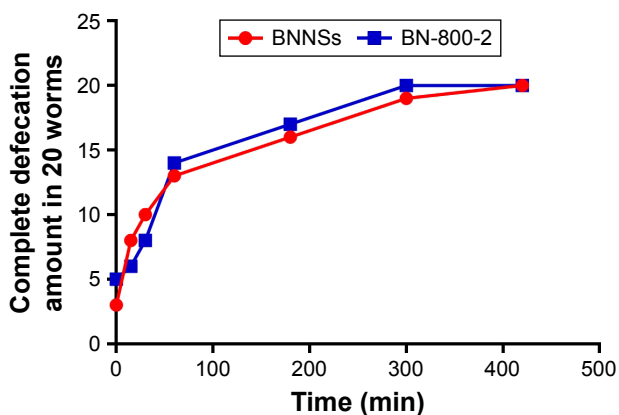
**Figure S2** The GABA nervous system in untreated control and BNNS- and BN-800-2-exposed worms.

**Notes:** (A) BNNSs or BN-800-2 ( $500 \mu\text{g}\cdot\text{mL}^{-1}$ ) were used to treat L4-stage larvae whose GABA motor neurons expressed a GFP construct (*oxIs12*) driven by a GABA motor neuron-specific promoter ( $n=30$ ). The worms were cultured in K medium without food for 24 hours during the treatment. Arrows indicate the position of D-type neurons in the control. Inset images are enlargements of regions outlined by small boxes. (B) Quantification of fluorescence intensity in worms treated as described in A. Data presented as means  $\pm$  SEM. \*\* $p<0.01$ . Scale bar  $100 \mu\text{m}$ .

**Abbreviations:** BNNSs, boron nitride nanospheres; BN-800-2, highly water-soluble boron nitride; GABA,  $\gamma$ -aminobutyric acid; SEM, standard error of mean.

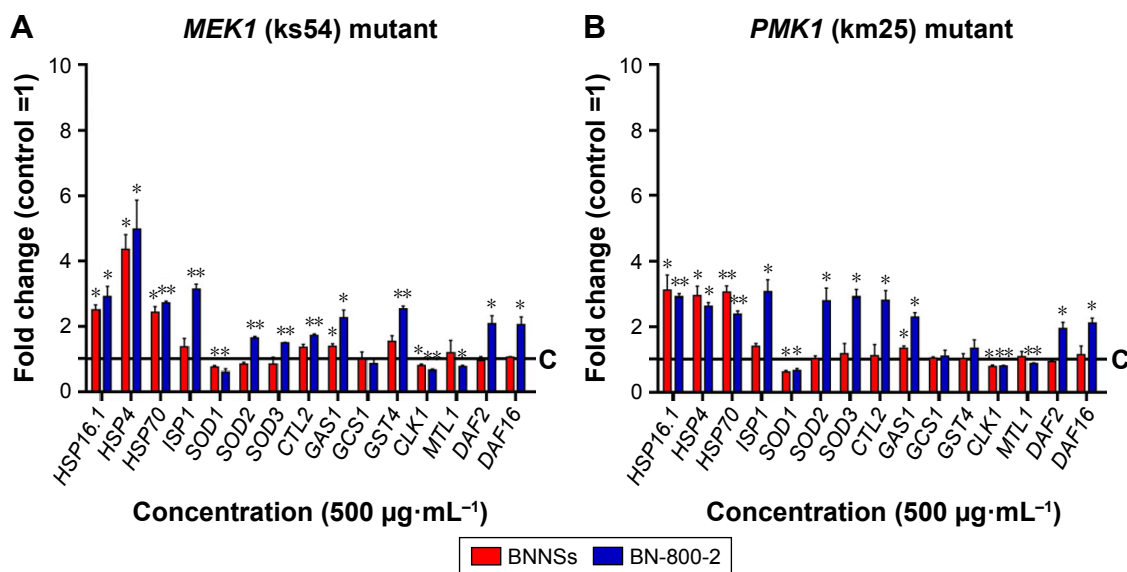
**Table S1** Information on genes related to stress response in *Caenorhabditis elegans*

Gene	Gene products
HSP4	GRP78/BiP homologous
HSP70	Heat-shock protein
HSP16.1	Heat-shock protein
ISP1	Rieske iron-sulfur protein
SOD1	Copper/zinc superoxide dismutase
SOD2	Iron/manganese superoxide dismutase
SOD3	Iron/manganese superoxide dismutase
CTL2	Catalase
GAS1	Subunit of mitochondrial complex I
MTL1	Metallothioneins
MTL2	Metallothioneins
GCS1	$\gamma$ -Glutamine cysteine synthetase heavy chain
GST4	Glutathione-requiring prostaglandin D synthase
CLK1	Ubiquinone biosynthesis protein COQ7
ETS4	Orthologue of E26 transformation-specific transcription factor
DAF2	Insulin/IGF-receptor orthologue
DAF16	Forkhead box O homologue
HSF1	Heat-shock transcription factor
SKN1	bZip transcription factor
MEK1	Mitogen-activated protein kinase kinase
PMK1	Mitogen-activated protein kinase
SEK1	Ortholog of human MAP2K3 and MAP2K6
VHP1	A MAP kinase phosphatase
BAR1	$\beta$ -Catenin
HMP2	$\beta$ -Catenin
AKT1	Serine/threonine kinase
GSA1	Heterotrimeric guanine nucleotide-binding protein
LAG1	C-promoter-binding factor and suppressor of hairless orthologue
SEL8	Glucagon-like peptide 1 and LIN12 signaling-required nuclear protein
EFN2	Orthologue of human ephrin-B3

**Figure S3** Defecation kinetics of worms after BN exposure.

**Notes:** Worms were subjected to 24-hour exposure to RhoB-labeled BNNSs and BN-800-2 (500  $\mu\text{g}\cdot\text{mL}^{-1}$ ) in K medium ( $n=20$ ). After exposure, the worms were washed and transferred to a clean plate for defecation in the absence of food. Complete defecation was defined as no RhoB-labeled BN materials observed in whole intestinal lumen of worms, the amount of which was recorded at 0, 15, and 30 minutes and 1, 3, 5, and 7 hours from transference. Data presented as mean  $\pm$  SD.

**Abbreviations:** BNNSs, boron nitride nanospheres; BN-800-2, highly water-soluble boron nitride; RhoB, rhodamine B.

**Figure S4** mRNA expression of oxidative stress-response genes in BNNS- or BN-800-2-exposed *MEK1* and *PMK1* mutant *Caenorhabditis elegans*.

**Notes:** The relative expression of genes related to oxidative stress response in *MEK1* (A) and *PMK1* (B) mutant *C. elegans* with exposure to BNNSs or BN-800-2 at a concentration of 500  $\mu\text{g}\cdot\text{mL}^{-1}$  for 24 hours. Three experimental repeats (three technical replicates for each experiment); C, control. All mRNA levels were normalized to *ACT1* mRNA levels and expressed as fold change relative to the untreated control. All experiments were done by exposing L4-stage larvae to BNNSs or BN-800-2 in K medium in 24-well plates at 20°C. Data presented as means  $\pm$  SEM. \* $P<0.05$ ; \*\* $P<0.01$ .

**Abbreviations:** BNNSs, boron nitride nanospheres; BN-800-2, highly water-soluble boron nitride; SEM, standard error of mean.



**International Journal of Nanomedicine****Dovepress****Publish your work in this journal**

The International Journal of Nanomedicine is an international, peer-reviewed journal focusing on the application of nanotechnology in diagnostics, therapeutics, and drug delivery systems throughout the biomedical field. This journal is indexed on PubMed Central, MedLine, CAS, SciSearch®, Current Contents®/Clinical Medicine,

Journal Citation Reports/Science Edition, EMBase, Scopus and the Elsevier Bibliographic databases. The manuscript management system is completely online and includes a very quick and fair peer-review system, which is all easy to use. Visit <http://www.dovepress.com/testimonials.php> to read real quotes from published authors.

Submit your manuscript here: <http://www.dovepress.com/international-journal-of-nanomedicine-journal>